Articles

Contribution from the Christopher Ingold Laboratories, University College London, London WC1H 0AJ, U.K., and Department of Chemistry, Queen Mary College, London E1 4NS, U.K.

Binuclear Platinum Diphosphite Complexes: X-ray Crystal Structures of $K_4[Pt_2(pop)_4Cl]\cdot 3H_2O$ and $K_4[Pt_2(pop)_4Br_2]\cdot 2H_2O$ (pop = $P_2O_5H_2^{2-}$)

Robin J. H. Clark,*† Mohamedally Kurmoo,† Helen M. Dawes,‡ and Michael B. Hursthouse‡

Received April 22, 1985

The structures of the complexes $K_4[Pt_2(pop)_4Cl]\cdot 3H_2O$ and $K_4[Pt_2(pop)_4Br_2]\cdot 2H_2O$, pop = $P_2O_5H_2^{2-}$, have been determined. Both are tetragonal. The chloride has cell dimensions $a = b = 13.249$ (2) Å, $c = 8.146$ (1) Å, space group $P4/mbm$ with two formula units per cell. The dibromide has cell dimensions $a = b = 9.483$ (4) Å, $c = 15.672$ (4) Å, space group $I4/mmm$ with two formula units per cell. The structure of the former consists of a linear chain with a $\cdots Pt^{II}\cdots Pt^{III}$–Cl polar repeating unit in the chain direction, the platinum atom pairs being bridged by four diphosphite (pop) ligands. The chains are disordered over the two possible directions leading to an averaged $\cdots Cl/2\cdots[Cl/2\cdots(Pt^{II}+Pt^{III})/2\cdots(Pt^{II}+Pt^{III})/2\cdots Cl/2]\cdots Cl/2\cdots$ crystallographic repeating unit. The Pt–Pt, Pt^{III}–Cl, and $Pt^{II}\cdots$Cl distances are 2.813 (1), 2.367 (7), and 2.966 (8) Å, respectively. The structure of $K_4[Pt_2(pop)_4Br_2]\cdot 2H_2O$ consists of discrete binuclear anions, with Pt–Pt and Pt–Br distances of 2.723 (4) and 2.555 (5) Å, respectively. The structure determinations complement other crystallographic and spectroscopic work on related complexes involving close stacking of binuclear units.

Introduction

Recent investigations of the products of partial oxidation of $[Pt_2(pop)_4]^{4-}$, pop = $P_2O_5H_2^{2-}$, with halogen have led to the isolation of metallic gold crystals of complexes $K_4[Pt_2(pop)_4X]\cdot nH_2O$, where X = Cl, Br, or I.[1] The X-ray crystal structure of the bromide[1] demonstrates that it consists of linear –Pt–Pt–X–Pt–Pt–X– chains, the Pt atoms being linked pairwise by four pop bridges. The chains provide an effective pathway for electrical conductivity since the chain conductivity is (5×10^{-4})–10^{-3} Ω^{-1} cm^{-1} for the powder, a high value for a halogen-bridged species. Complementary spectroscopic (in particular, resonance Raman) results on these and related complexes[2,3] have called into question one crystallographic feature of this structure, namely, that of central bromine atom bridging between the $Pt_2(pop)_4$ units, viz.

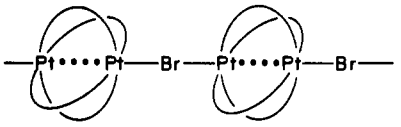

Although this feature would favor high chain conductivity, it would be inconsistent with both the expected Peierl's instability of symmetric linear chains and also the observed Raman activity[2] of the symmetric Pt–Br stretching mode. Accordingly, we have investigated the X-ray crystal structure of $K_4[Pt_2(pop)_4Cl]\cdot 3H_2O$ and shown conclusively that, at least in this complex, the bridging halogen atom is not centrally placed between the Pt_2 units, despite its crystallizing in the same space group as the analogous bromide. Detailed comparisons of the two structures are made, together with detailed comparisons of the structures of $K_4[Pt_2(pop)_4]\cdot 2H_2O$,[4,5] $K_4[Pt_2(pop)_4Cl_2]\cdot 2H_2O$,[1] and $K_4[Pt_2(pop)_4Br_2]\cdot 2H_2O$, the results on the last complex being also reported herein.

Experimental Section

The complexes ($K_4[Pt_2(pop)_4Cl]\cdot 3H_2O$, metallic gold crystals, and $K_4[Pt_2(pop)_4Br_2]\cdot 2H_2O$, orange crystals) were prepared as described in ref 1 and 2.

Crystallographic Studies. Intensity data were collected on a Nonius CAD4 diffractometer to a θ maximum of 25° (graphite-monochromated Mo Kα radiation) using the ω–2θ scan mode and were corrected for absorption empirically.[6] An additional correction for absorption (DIFABS)[7] was applied during refinement. A common 20% decrease in intensity of the three standard reflections monitored during data collection was observed for $K_4[Pt_2(pop)_4Br_2]\cdot 2H_2O$, and the data were scaled for isotropic decay.

Crystal data are specified in Table I, while details of methods used for data collection have been given in a prior publication.[8] All compu-

Table I. Crystal Data and Details of Structure Analyses

	$K_4[Pt_2(pop)_4Cl]\cdot 3H_2O$	$K_4[Pt_2(pop)_4Br_2]\cdot 2H_2O$
M_r	1229.94	1318.28
cryst syst	tetragonal	tetragonal
a/Å	13.249 (2)	9.483 (4)
b/Å	13.249 (2)	9.483 (4)
c/Å	8.146 (1)	15.672 (4)
V/Å^3	1429.7	1409.3
space group	$P4/mbm$	$I4/mmm$
Z	2	2
ρ_c/g cm^{-3}	2.86	3.11
$F(000)$	1122	1172
μ(Mo Kα)/cm^{-1}	105.25	133.64
cryst size/mm	0.25 × 0.28 × 0.30	0.12 × 0.20 × 0.25
θ range/deg; octant	1.5–25; $+h,+k,+l$	1.5–25; $+h,+k,+l$
no. of unique data	727	399
no. of obsd data	622	375
significance test	$F > 3\sigma(F)$	$F > 3\sigma(F)$
no. of params	61	34
weighting scheme coeff g in $\omega = 1/[\sigma^2(F_o)+gF_o^2]$	0.0001	0.000 08
final $R = \sum\Delta F/\sum\lvert F_o\rvert$	0.0256	0.0292
$R' = (\sum\omega\Delta F^2/\sum\omega F_o^2)^{1/2}$	0.0318	0.0396

† University College London.
‡ Queen Mary College.

(1) Chê, C.-M.; Herbstein, F. H.; Schaefer, W. P.; Marsh, R. E.; Gray, H. B. *J. Am. Chem. Soc.* **1983**, *105*, 4604–4607.
(2) Kurmoo, M.; Clark, R. J. H. *Inorg. Chem.* **1985**, *24*, 4420–4425.
(3) Clark, R. J. H.; Kurmoo, M. *J. Chem. Soc., Dalton Trans.* **1985**, 579–585.
(4) Filomena Das Remedios Pinto, M. A.; Sadler, P. J.; Neidle, S.; Sanderson, M. R.; Subbiah, A.; Kuroda, R. J. *J. Chem. Soc., Chem. Commun.* **1980**, 13–15.
(5) Marsh, R. E.; Herbstein, F. H. *Acta Crystallogr., Sect. B: Struct. Sci.* **1983**, *B39*, 280–287.
(6) North, A. C. T.; Philips, D. C.; Mathews, F. S. *Acta Crystallogr., Sect. A: Cryst. Phys., Diffr., Theor. Gen. Crystallogr.* **1968**, *A24*, 351–359.
(7) Walker, N.; Stuart, D. *Acta Crystallogr., Sect. A: Found. Crystallogr.* **1983**, *A39*, 158–162.

0020-1669/86/1325-0409$01.50/0

Table II. Fractional Atomic Coordinates ($\times 10^4$) for $K_4[Pt_2(pop)_4Cl]\cdot 3H_2O$

	x	y	z
Pt	0	0	3273 (0.5)
Cl	0	0	-368 (6)
P	1186 (1)	1298 (1)	3195 (1)
O(1)	2165 (3)	1030 (3)	2193 (5)
O(2)	837 (3)	2323 (3)	2591 (5)
O(3)	1665 (4)	1486 (4)	5000
K(1)	2264 (2)	2736 (2)	0
K(2)	1122 (1)	3878 (1)	5000
W(1)	3994 (6)	1006 (6)	4678 (37)[a]
W(2)	4496 (18)	0504 (18)	2744 (50)[b]

[a] Half-occupancy of site. [b] One-fourth occupancy of site.

tations were carried out by using SHELX76[9] on a DEC VAX 11/750.

Solution to, and Refinement of, the Structure of $K_4[Pt_2(pop)_4Cl]\cdot 3H_2O$. Diffractometer intensity measurements confirmed the crystal system as tetragonal, Laue group *P4/mmm*. Three possible space groups, *P4bm*, $P\bar{4}b2$, and *P4/mbm* were consistent with the systematic absences $0kl$, $k \neq 2n$. The centrosymmetric space group *P4/mbm* was initially selected on the basis of the statistics and the results obtained by Chē *et al.* for the analogous bromide.[1] A Patterson function was interpreted to give a platinum atom on a 4-fold axis; a chlorine atom with site symmetry *4/m* was fixed arbitrarily at the origin. The remaining atomic positions located were in accordance with those in the bromide structure. Electron intensity difference maps revealed two sites for water molecules, refinement suggesting W(1) and W(2) to be positioned on sites of symmetry *m*. The final model adopted involved one-half occupation by the former and one-fourth occupation by the latter, in agreement with the findings of Chē et al. on the analogous bromide. In the final stages of full-matrix least-squares refinement, with anisotropic temperature parameters for all atoms, a high degree of thermal motion along the *c* direction was indicated for the chlorine atom by the value (0.145 Å^2) of U_{33}. This atom was accordingly refined as occupying two sites (4-fold symmetry) on either side of the mirror plane at $z = 0$. A reduction of 0.11% in the *R* factor was achieved together with a significant reduction to 0.010 Å^2 for the U_{33} value. Hydrogen atoms were not included in the structure factor calculation.

In order to examine further the disorder/thermal motion problem affecting the chlorine atom position (and the interpretation of the structural results—see Discussion), attempts were made to recollect data (on a second crystal) at reduced temperatures. However, on cooling, the reflection peak widths began to increase, and so the temperature was lowered only to −20 °C. A data set comparable to that recorded at room temperature was collected, but, on interpretation, no significant differences in the structure were found, apart from a general decrease in thermal parameters by ~5–10% and some instability in the water oxygen atom refinement; this probably indicates differences in occupancy of the various sites from crystal to crystal. At this point, work on this data set was discontinued.

Solution to, and Refinement of, the Structure of $K_4[Pt_2(pop)_4Br_2]\cdot 2H_2O$. The crystal system was established to be tetragonal, Laue group *I4/mmm*. No systematic absences were noted in the data other than the *I* lattice absences, and so the space group *I4/mmm* was indicated. A platinum and a bromide atom were located at positions of site symmetry *4mm* from a Patterson map. In the phosphite ligand the phosphorus atom lies on a position of symmetry *m* while the bridging oxygen atom is situated at a position of *mm* symmetry. Refinement proceeded by full-matrix least squares with anisotropic thermal parameters for all atoms. The thermal ellipsoid of the phosphite bridging oxygen atom was found to be extensively elongated in a direction perpendicular to the plane of the ligand. Accordingly this atom was represented by two half-atoms sited on each side of the mirror plane. Subsequent electron density difference maps revealed two remaining regions of density, K(1) at a site with $\bar{4}m2$ symmetry and K(2) sharing alternate sites (*mm*) with a water molecule. Hydrogen atoms could not be located.

Results and Discussion

$K_4[Pt_2(pop)_4Cl]\cdot 3H_2O$. Final fractional atomic coordinates and occupancies are given in Table II for $K_4[Pt_2(pop)_4Cl]\cdot 3H_2O$, and the important bond lengths and angles and nonbonded distances are given in Tables III and IV, respectively.

Table III. Bond Lengths (Å) and Bond Angles (deg) for $K_4[Pt_2(pop)_4Cl]\cdot 3H_2O$[a]

Pt–Pt(a)	2.813 (1)	Pt–Cl	2.966 (8)
Pt–Cl(b)	2.367 (7)	Pt–P	2.329 (3)
O(1)–P	1.573 (6)	O(2)–P	1.516 (6)
O(3)–P	1.621 (5)		
Cl–Pt–Pt(a)	180.0	P–Pt–Pt(a)	91.6 (3)
P–Pt–Cl	88.4 (2)	P–Pt–P(b)	176.9 (1)
O(1)–P–Pt	113.8 (3)	O(2)–P–Pt	117.7 (3)
O(3)–P–Pt	110.7 (3)	O(2)–P–O(1)	106.6 (3)
O(3)–P–O(1)	100.5 (3)	O(2)–P–O(3)	106.0 (4)
P–O(3)–P	130.2 (4)		

[a] Key to symmetry operations relating designated atoms to reference atoms at (x, y, z): (a) $-x, -y, 1.0 - z$; (b) $-x, -y, -z$.

Table IV. Selected Nonbonded Distances (Å) for $K_4[Pt_2(pop)_4Cl]\cdot 3H_2O$[a]

W(2)–W(1)	1.834	K(1)–O(1)	2.884
W(1)–O(1)	3.156	W(2)–O(1)	3.198
K(2)–O(2)	2.871	K(1)–O(2)	2.886
K(2)–O(3)	3.249	W(1)–O(3)	3.161
O(1)–Cl(b)	3.506	O(2)–Cl(b)	3.739
O(3)–O(1)(c)	2.456	O(2)–O(1)(e)	2.502
K(1)–O(1)(h)	2.884	K(1)–O(1)(i)	2.884
W(1)–O(1)(i)	3.157	W(2)–O(1)(i)	3.198
K(2)–O(3)(g)	3.249	W(1)–O(3)(g)	3.162
K(2)–O(2)(c)	2.871	K(1)–O(2)(d)	2.886
K(2)–O(2)(g)	2.870	K(1)—O(2)(h)	2.886
K(2)–O(2)(i)	2.870	K(1)–O(2)(i)	2.886
K(1)–K(2)(j)	4.600	K(2)–K(2)(k)	4.206
W(1)K(2)(l)	2.836	W(2)–K(2)(l)	2.949
W(1)–K(2)(m)	2.837	W(2)–K(2)(m)	2.949
W(2)–W(1)(n)	3.238	W(2)–W(1)(c)	2.304
K(1)–O(1)(d)	2.884		
W(2)–W(2)(n)	1.888		

[a] Key to symmetry operations relating designated atoms to reference atoms at (x, y, z): (a) $-x, -y, 1.0 - z$; (b) $-x, -y, -z$; (c) $x, y, 1.0 - z$; (d) $x, y, -z$; (e) $-y, x, z$; (f) $y, -x, z$; (g) $0.5 - y, 0.5 - x, 1.0 - z$; (h) $0.5 - y, 0.5 - x, -z$; (i) $0.5 - y, 0.5 - x, z$; (j) $x, y, -1.0 + z$; (k) $-x, 1.0 - y, 1.0 - z$; (l) $0.5 + x, 0.5 - y, z$; (m) $0.5 - x, -0.5 + y, 1.0 - z$; (n) $1.0 - x, -y, z$.

The structure of $K_4[Pt_2(pop)_4Cl]\cdot 3H_2O$ is analogous to that of the bromide except in one important respect. The analysis shows that, in the chloride, the bridging atom is disordered over two sites in a manner analogous to that found for many Pt^{II}/Pt^{IV} mixed-valence chain complexes of the Wolffram's red sort.[10] There are, thus, alternate short (2.367 (7) Å) and long (2.966 (8) Å) Pt–Cl bonds in the chain direction, a result which is entirely in agreement with the resonance Raman results.[2] These indicate not only that the Pt–Cl stretching mode is strongly Raman active but also that, at resonance with the Pt^{II}/Pt^{III} intervalence band (512 nm), long progressions are observed in ν(PtCl) (291 cm^{-1}); neither of these spectroscopic results would obtain were the chlorine atoms centrally bridging between the $Pt_2(pop)_4$ units. The chain structure of the chloride can be interpreted in terms of two models, in both of which chain disorder is required. These models are constructed from one or other of the chains shown (a and b).

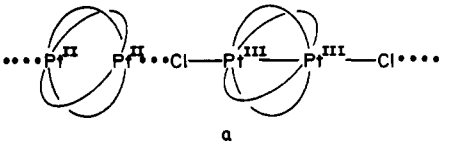

a

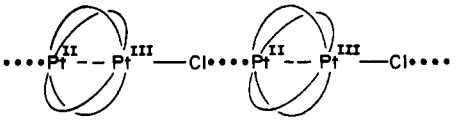

b

(8) Hursthouse, M. B.; Jones, R. A.; Malik, K. M. A.; Wilkinson, G. *J. Am. Chem. Soc.* **1979**, *101*, 4128–4139.
(9) Sheldrick, G. M. "SHELX 76", program for crystal structure determination, University of Cambridge, 1976.
(10) Clark, R. J. H. *Adv. Infrared Raman Spectrosc.* **1984**, *11*, 95–132.

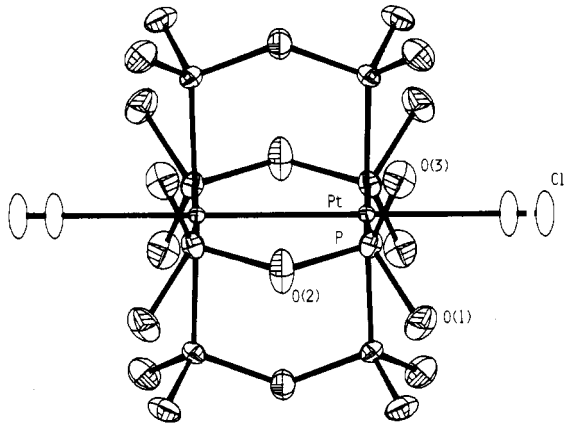

Figure 1. Diagram of the chain repeating unit in $K_4[Pt_2(pop)_4Cl]\cdot 3H_2O$, including the atom-numbering scheme.

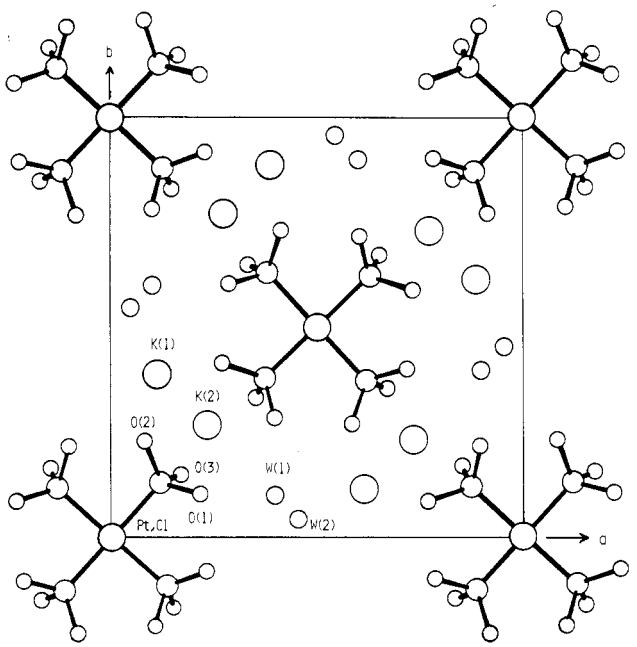

Figure 2. View of the unit cell contents down the chain axis (*c*).

Although against our initial prejudices, we favor a model composed of chains of type b for the following reasons. Previous structure determinations have yielded geometric parameters for the systems $[Pt^{II}_2(pop)_4]^{4-}$[4,5] and $[Pt^{III}_2(pop)_4Cl_2]^{4-}$,[1] in which the Pt–Pt distances are quite different from one another, at 2.925 (1) and 2.695 (1) Å, respectively. A structure based on chain type a would therefore involve disorder of dimers with quite different Pt–Pt lengths and would be expected to show either split or considerably elongated peaks for the Pt atoms. This is certainly not the case in our structure since the Pt U_{33} parameter has a value of 0.009 Å^2 and the largest electron density ripple near the Pt site had a density of only 0.5 e Å^{-3}.

The use of these model requires the acceptance of certain other criteria. We must presume that the packing of the dimers is controlled solely by the $[Pt_2(pop)_4]$ units, and that the equatorial geometries around the Pt^{II} and Pt^{III} centers must be extremely similar to one another. That this is reasonable is again supported by the situation found in the Pt^{II}/Pt^{IV} Wolffram's red salt structures, where chain disorder also occurs. The chain structure found is illustrated in Figure 1, and a packing diagram is given in Figure 2.

The geometry of the pop ligand is similar to that found for the earlier structures. The two terminal P–O distances (typical of those in phosphites and pyrophosphites) show a small difference of ~0.05 Å and may correspond to localization into "P=O" and "P—OH" units as suggested by Chê et al.[1] The P–O–P angle of 130.2 (4)° lies between that found for the Pt^{II}_2 and $Pt^{III}_2Cl_2$ systems (133.3 (9) and 125.5 (4)°), respectively and agrees exactly with the value of 130.2 (3)° found[1] for $K_4[Pt_2(pop)_4Br]\cdot 3H_2O$. Clearly this bond angle is strongly dependent on the Pt–Pt distance, which is similar in the two chain structures (2.813 (1) and 2.793 (1)[1] Å for X = Cl or Br, respectively).

Table V. Fractional Atomic Coordinates (×10^4) for $K_4[Pt_2(pop)_4Br_2]\cdot 2H_2O$

	x	*y*	*z*
Pt	0	0	869 (0.5)
Br(1)	0	0	2499 (1)
P	2468 (3)	0	921 (1)
O(1)	3138 (5)	1289 (5)	1345 (4)
O(2)	3116 (12)	485 (12)	0
K(1)	5000	0	2500
K(2)	5000	2657 (8)	0
W(1)	5000	2657 (8)	0

Table VI. Bond Lengths (Å) and Bond Angles (deg) for $K_4[Pt_2(pop)_4Br_2]\cdot 2H_2O$[a]

Pt–Pt(a)	2.723 (4)	Pt–Br(1)	2.555 (5)
Pt–P	2.342 (4)	O(1)–P	1.529 (7)
O(2)–P	1.635 (8)		
Br(1)–Pt–Pt(a)	180.0	P–Pt–Pt(a)	92.0 (2)
P–Pt–Br(1)	88.0 (2)	P–Pt–P(b)	176.0 (1)
O(1)–P–Pt	115.5 (3)	O(2)–P–Pt	110.2 (5)
O(2)–P–O(1)	90.2 (5)	O(1)–P–O(1)(c)	106.0 (5)
P–O(2)–P	124.0 (8)		

[a] Key to symmetry operations relating designated atoms to reference atoms at (*x*, *y*, *z*): (a) $-x, -y, -z$; (b) $-x, -y, z$; (c) y, x, z.

Table VII. Selected Nonbonded Distances (Å) for $K_4[Pt_2(pop)_4Br_2]\cdot 2H_2O$[a]

O(1)–K(1)	2.808	K(2)–K(1)	4.658
K(2)–O(1)	3.041	W(1)–O(1)	3.041
W(1)–O(2)	2.727	K(2)–O(2)	2.727
K(2)–Br(1)(a)	4.505	K(1)–Br(1)(b)	4.740
K(2)–Br(1)(c)	4.505	K(2)–K(1)(d)	4.658
O(2)–O(1)(e)	2.242	K(2)–O(1)(e)	3.041
W(1)–O(1)(e)	3.041	K(2)–O(1)(f)	3.041
W(1)–O(1)(f)	3.041	O(2)–O(1)(g)	2.697
O(1)–O(1)(h)	2.443	O(2)–O(1)(h)	2.697
K(2)–O(1)(i)	3.041	W(1)–O(1)(i)	3.041
K(2)–O(1)(j)	4.129	K(2)–O(1)(k)	4.129
O(1)–O(1)(l)	2.480	K(2)–O(1)(l)	4.129
K(2)–O(1)(m)	4.129	K(2)–O(2)(d)	3.474
K(2)–O(2)(f)	2.727	W(1)–O(2)(f)	2.727
K(2)–O(2)(g)	3.474	K(2)–K(2)(n)	4.443
W(1)–K(2)(j)	3.142	W(1)–K(2)(o)	3.142
W(1)–W(1)(j)	3.142	W(1)–W(1)(o)	3.142
K(2)–K(2)(j)	3.142	K(2)–K(2)(o)	3.142

[a] Key to symmetry operations relating designated atoms to reference atoms at (*x*, *y*, *z*): (a) $0.5 + x, 0.5 + y, -0.5 + z$; (b) $0.5 - x, -0.5 - y, 0.5 - z$; (c) $0.5 - x, 0.5 - y, 0.5 - z$; (d) $1.0 - x, -y, -z$; (e) $x, y, -z$; (f) $1.0 - x, y, z$; (g) $x, -y, -z$; (h) $x, -y, z$; (i) $1.0 - x, y, -z$; (j) $1.0 - y, x, z$; (k) $1.0 - y, x, -z$; (l) y, x, z; (m) $y, x, -z$; (n) $1.0 - x, 1.0 - y, -z$; (o) $y, 1.0 - x, -z$.

$K_4[Pt_2(pop)_4Br_2]\cdot 2H_2O$. Final fractional atomic coordinates and occupancies are given in Table V for $K_4[Pt_2(pop)_4Br_2]\cdot 2H_2O$, and important bond lengths and angles and nonbonded distances are given in Tables VI and VII, respectively.

The crystal structure of the dibromide is, surprisingly, quite different from that of the dichloride.[1] The dibromide adopts a structure in which the $[Pt_2(pop)_4Br_2]^{4-}$ unit has very high, 4/*mmm*, symmetry. As a consequence, the pop ligand is "constrained" to lie on a mirror plane, although the structure refinement in which the bridging oxygen atom was shown to half-occupy two sites indicates that this result is achieved by disorder of a folded P–O–P system, as has been found for all other pop structures. The disorder is also reflected in large thermal ellipsoids for the terminal "P=O, P—OH" oxygen atoms. A view of $[Pt_2(pop)_4Br_2]^{4-}$ is shown in Figure 3, and the cell contents are shown in Figure 4.

Table VIII. Selected Bond Distances and Angles for Potassium Salts of Platinum Diphosphite Complexes

	$K_4[Pt_2(pop)_4]\cdot 2H_2O$[a]	$K_4[Pt_2(pop)_4Cl]\cdot 3H_2O$[b]	$K_4[Pt_2(pop)_4Br]\cdot 3H_2O$[c]	$K_4[Pt_2(pop)_4Cl_2]\cdot 2H_2O$[c]	$K_4[Pt_2(pop)_4Br_2]\cdot 2H_2O$[b]
			Bond Distance (Å)		
Pt–Pt	2.925 (1)	2.813 (1)	2.793 (1)	2.695 (1)	2.723 (4)
Pt–P	2.320 (5)	2.329 (3)	2.334 (1)	2.350 (2)	2.342 (4)
Pt—O(H)	1.579 (9)	1.573 (6)	1.562 (4)	1.557 (7)	1.529 (7)
P=O	1.519 (9)	1.516 (6)	1.505 (4)	1.512 (7)	1.529 (7)
P—O(br)	1.623 (6)	1.621 (5)	1.618 (3)	1.616 (7)	1.635 (8)
Pt—X		2.367 (7)	2.669 (1)	2.407 (2)	2.555 (5)
		2.966 (8)			
P···P	2.980 (6)	2.946 (6)	2.935 (2)	2.873 (3)	2.887 (7)
O(H)···O	2.505 (19)	2.497 (8)	2.487 (5)	2.486 (9)	2.480 (9)
			Bond Angle (deg)		
Pt—Pt—P	90.67 (10)	91.6 (3)	91.74 (2)	92.17 (5)	92.0 (2)
Pt—P—O(H)	114.0 (5)	113.8 (3)	113.4 (1)	113.9 (3)	110.2 (5)
Pt—P=O	118.0 (5)	117.7 (3)	117.3 (2)	115.7 (3)	115.5 (3)
Pt—P—O(br)	110.3 (4)	110.7 (3)	110.4 (2)	110.2 (3)	110.2 (5)
P—O—P	133.3 (9)	130.2 (4)	130.2 (3)	125.5 (4)	124.0 (8)
Pt—Pt—X		180.0 (1)	180.0 (1)	179.0 (1)	180.0 (1)

[a] References 4 and 5. [b] This work. [c] Reference 1.

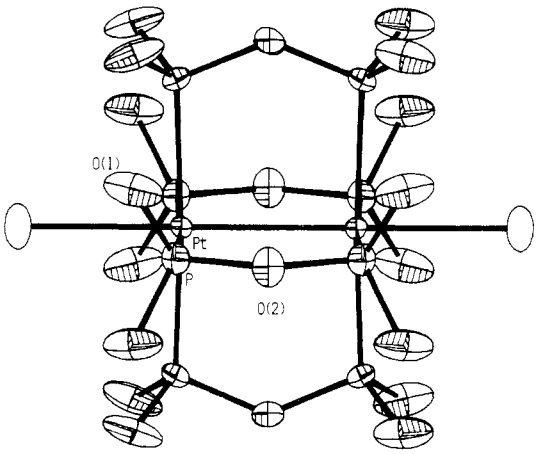

Figure 3. Diagram of the dimer in $K_4[Pt_2(pop)_4Br_2]\cdot 2H_2O$, including the atom-numbering scheme.

The Pt–Pt distance in $[Pt_2(pop)_4Br_2]^{4-}$ (2.723 (4) Å) is similar to that found for the analogous chloride (2.695 (1) Å).[1] The average Pt^{III}–Pt^{III} distance in these two structures (2.709 Å) is less than the average Pt^{II}–Pt^{III} distance in the two chain structures (2.803 Å), which in turn is less than the $Pt^{II}\cdots Pt^{III}$ distance in $[Pt_2(pop)_4]^{4-}$ (2.925 (1) Å). This result, as pointed out by Che et al.[1], is consistent with the electronic structural model in which the Pt^{III}–Pt^{III}, Pt^{II}–Pt^{III} and Pt^{II}–Pt^{II} complexes have the electronic configurations d_σ^2, $d_\sigma^2 d_{\sigma^*}^1$, and $d_\sigma^2 d_{\sigma^*}^2$, respectively, and Pt–Pt bond orders of 1, $^1/_2$, and 0, respectively.

The Pt–Br distance in this structure (2.555 (5) Å) is substantially longer than that of a normal single bond (2.43 Å),[11] implying that a Pt–Pt structural trans effect is present. The other bond lengths and angles in this structure are closely similar to those in $[Pt_2(pop)_4Cl_2]^{4-}$. A detailed comparison of five different pop structures is given in Table VIII.

Conclusion

The structure of $K_4[Pt_2(pop)_4Cl]\cdot 3H_2O$ marks it out as a localized-valence (Pt^{II}/Pt^{III}) species on account of the fact that the chain Pt–Cl distances (2.367, 2.966 Å) differ substantially (by 0.60 Å). In this respect, the complex shows close similarities to Wolffram's red type salts, for which chain Pt^{IV}–Cl distances for seven structures cover the range 2.30 ± 0.04 Å while the chain

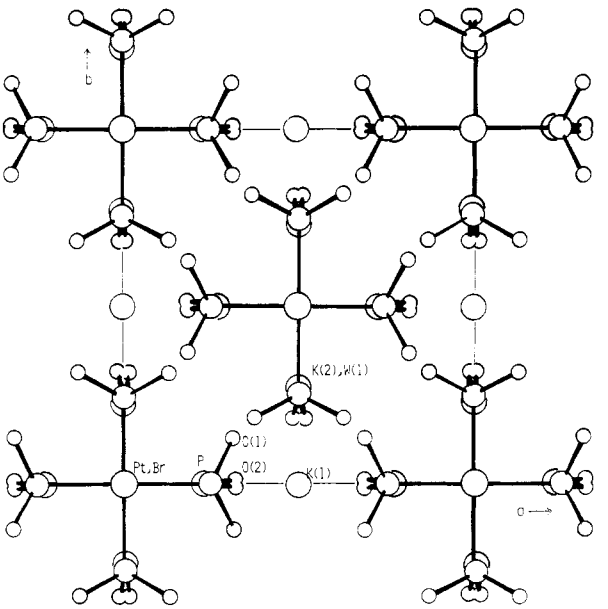

Figure 4. View of the unit cell contents down the *c* axis.

Pt^{II}–Cl distances cover the range 3.06 ± 0.23 Å.[10] Both crystallographic[1] and spectroscopic[2] results indicate that the analogous bromide and iodide are much nearer to being delocalized-valence species (as indeed are the bromide and iodide versions of Wolffram's red type salts).[10] However, the spectroscopic results[2] indicate that even for these two complexes the halogen atom is not bridging exactly centrally, as stated in ref 1. The bromide and iodide are thus in both structures and properties closely similar to the dithioacetate complex $Pt_2(CH_3CS_2)_4I$, which is likewise a semiconductor with nearly but not exactly equal chain Pt–I bond lengths of 2.975 and 2.981 Å.[12]

Acknowledgment. The authors thank the SERC for financial support and Johnson Matthey P.L.C. for the loan of chemicals.

Registry No. $K_4[Pt_2(pop)_4Cl]\cdot 3H_2O$, 99632-90-3; $K_4[Pt(pop)_4Br_2]\cdot 2H_2O$, 99632-91-4.

Supplementary Material Available: Listings of observed and calculated structure factors for the two complexes and anisotropic temperature factors (8 pages). Ordering information is given on any current masthead page.

(11) Wells, A. F. "Structural Inorganic Chemistry"; 5th ed.; Clarendon Press: Oxford, England, 1984.

(12) Bellito, C.; Flamino, A.; Gastaldi, L.; Scaramuzza, L. *Inorg. Chem.* **1983**, *22*, 444–449.